

# Speeding Up Computer Simulations: The Transition Observable Method

M. Kastner and M. Promberger

Institut für Theoretische Physik, Universität Erlangen-Nürnberg, Staudtstrasse 7, D-91058  
Erlangen, Germany

J.D. Muñoz

ICA1 Universität Stuttgart, Pfaffenwaldring 27, D-70569 Stuttgart, Germany

Permanent address: Departamento de Física, Universidad Nacional de Colombia, Bogota D.C.,  
Colombia  
(May 18, 2019)

## Abstract

A method is presented which allows for a tremendous speed-up of computer simulations of statistical systems by orders of magnitude. This speed-up is achieved by means of a new observable, while the algorithm of the simulation remains unchanged.

## I. INTRODUCTION

In performing a Monte Carlo simulation, one or several observables are chosen, for which a simulation average is recorded. A common choice for such an observable is related to a histogram as introduced by Salzburg [1] and popularized by Swendsen and Ferrenberg [2], [3]. The histogram allows for the estimation of the density of states, from which a variety of physically interesting system properties can be computed. Recently, Oliveira et al. [4] suggested a new method, called transition observable method throughout this paper, which likewise enables an estimation of the density of states but leads to considerable reduction of the computing time. In other words, the simulation may be dramatically accelerated without modifying the algorithm but by changing the observable recorded during the simulation.<sup>1</sup>

If the standard histogram method is applied to magnetic systems, the number of microstates with energy  $E$  and magnetization  $M$  is counted during the course of simulation, i.e., every microstate yields one entry in an energy-magnetization histogram. From this histogram the density of states can be computed (cf. Sec. II C).

In the transition observable method, each microstate of the Monte Carlo sample is exploited in a much more sophisticated way. For the particular realization of the method introduced in Sec. III, this means: In an extended histogram, the number of possible transitions is recorded from particular microstates (in the Monte Carlo sample) with energy  $E$  and magnetization  $M$  to "neighbouring" microstates (not necessarily in the Monte Carlo sample) with energy  $E - E$  and magnetization  $M - M$ , which can be reached from the particular microstates of the sample by applying single spin flip operations. Again, from this extended histogram, the density of states can be computed (cf. Sec. II D).

As already pointed out by Oliveira [6], the advantage of the transition observable method is that every microstate of the Monte Carlo sample is investigated much more extensively than by the standard histogram technique. Therefore, given a certain sample of microstates, the density of states can be calculated more accurately from simulation averages of the transition observable introduced below than by standard methods. Additionally, as it is the selection of microstates using pseudo random numbers which is costly in computing time, the increase in computing time from such a more extensive exploration of the chosen microstates is absolutely negligible<sup>2</sup>. However, the effect on the data quality is significant and can amount to orders of magnitude. In the case of the examples studied in this paper, we find an efficiency gain of roughly two orders of magnitude! This efficiency gain can be expected to grow proportional to  $L^{d=2}$ , the square root of the volume of the system.

It is this enormous gain of efficiency which should motivate the reader to occupy himself with the underlying formalism, which is indeed simple to implement in a simulation, but is somewhat heavy to formalize.

Section II A and II B aim to familiarize the reader with the language used throughout this paper and with some aspects of the Monte Carlo procedure. In section II C, the standard

---

<sup>1</sup> Since this new observable represents properties of the system under consideration, it is of course completely independent of the particular simulation setup.

<sup>2</sup> At least in the case of the particular realization of the method introduced below.

histogram technique is reviewed in the context of the calculation of the density of states. The transition observable is introduced in Sec. II D. In Sec. II E, it is shown that this observable includes the one presented in reference [5] as a special case. The rest of the paper (section III) is devoted to the comparison of the efficiency of computer simulations using the new method in contrast to a standard histogram technique. This is done for the examples of 2d- and 3d-Ising systems where we find a speed-up factor of 40 in the  $32^2$  Ising system and 250 in the  $10^3$  Ising system.

## II. CALCULATING THE DENSITY OF STATES BY MONTE-CARLO SIMULATION

### A. Conventions and notation

In this paper, we use the language of discrete Ising systems on hypercubic lattices of linear size  $L$  in  $d$  spatial dimensions with Hamiltonian

$$\begin{aligned} H(S) &= \sum_{i,j} h_{i,j} S_i S_j \\ &= :E(S) - hM(S); \quad S \in \{-1, 1\}^L; \end{aligned} \quad (1)$$

where  $h$  denotes an external magnetic field.  $E(S)$  is the interaction energy and  $M(S)$  the magnetization of the particular microstate  $S = (S_1, S_2, \dots, S_L)$  (particular configuration of the spins  $S_i$ ,  $i = 1, 2, \dots, L$  on the  $L^d$  lattice) with  $S_i \in \{-1, 1\}$ . The configuration space of the Ising system is denoted by  $\mathbb{S}^L$ , and  $h_{i,j}$  indicates a summation over all pairs of nearest neighbours.

The discreteness of the Ising system gives rise to a minimal energy and magnetization spacing, denoted by  $E$  and  $M$ , respectively. Summations over interaction energy  $E$  (magnetization  $M$ ) cover all energy (magnetization) values accessible.

In general, in order to simplify the notation, system size dependencies are not stated explicitly. In what follows, all energies are measured in units of the Ising coupling constant  $J$ , all temperatures in units of  $J=k_B$  ( $k_B$  : Boltzmann's constant).

### B. Some remarks on Monte-Carlo simulations

For a Monte Carlo simulation, a Markov process is set up on configuration space  $\mathbb{S}^L$  with a certain problem adapted stationary distribution  $\hat{w}(S)$ , which is assumed<sup>3</sup> to depend only on the interaction energy  $E$  and the magnetization  $M$  of the microstate  $S$ , i.e.  $\hat{w}(S) = w(E(S); M(S))$ . From the Markov chain  $\{S_N\}$  of length  $N$  (which, at least in the limit of

---

<sup>3</sup>It is straightforward to extend the formalism introduced in the following sections to the case of a more general stationary distribution. The restricting assumption  $\hat{w}(S) = w(E(S); M(S))$  is made only for the sake of notational simplicity.

in nitely long samples, is distributed according to  $w$ ) the simulation average of an arbitrary function  $f : \mathbb{L}^d \rightarrow \mathbb{R}$  on configuration space is obtained:

$$hf(S) \hat{i}_{\text{sim}, w}(fSg_N) := \frac{1}{N} \sum_{S \in \mathbb{L}^d} f(S) \frac{N!}{S!} \sum_{S \in \mathbb{L}^d} f(S) w(S) : \quad (2)$$

Of course, the simulation average depends on the stationary distribution and, unless the length of the Markov chain reaches infinity, on the particular sample  $fSg_N$ .

### C. Standard histogram technique

The histogram  $H_w(E; M; fSg_N)$ , which is proportional to the number of microstates of the sample with interaction energy  $E$  and magnetization  $M$ , is given by the simulation average of the observable  $E(S); E(M(S); M)$ :

$$\begin{aligned} H_w(E; M; fSg_N) &= \sum_{S \in \mathbb{L}^d} E(S); E(M(S); M) \hat{i}_{\text{sim}, w}(fSg_N) \\ &= \frac{1}{N} \sum_{S \in \mathbb{L}^d} E(S); E(M(S); M) \\ &\quad \frac{N!}{S!} \sum_{S \in \mathbb{L}^d} E(S); E(M(S); M) w(E(S); M(S)) \\ &= \langle E; M \rangle w(E; M) : \end{aligned} \quad (3)$$

Since the underlying stationary distribution  $w$  is known (at least beside an irrelevant factor), the density of states is obtained as

$$\begin{aligned} \langle E; M \rangle &= \sum_{S \in \mathbb{L}^d} E(S); E(M(S); M) \\ &= \lim_{N! \rightarrow 1} H_w(E; M; fSg_N) / w(E; M) ; \end{aligned} \quad (4)$$

or | more realistically for a computer simulation | at least an estimator for  $\langle E; M \rangle$  is obtained by omitting the limiting procedure  $\lim_{N! \rightarrow 1}$ .

### D. Transition observable method

In this section it is shown that the density of states can be obtained from simulation averages of certain transition observables defined below, which have the advantageous feature that they enable the estimation of the density of states in a much more efficient way than the standard histogram method does.

As a preliminary step, let us define the microcanonical average of any system observable  $f(S)$ :

$$\begin{aligned} hf(S) \hat{i}(E; M) &= \lim_{\substack{N! \rightarrow 1 \\ P}} \frac{\sum_{S \in \mathbb{L}^d} f(S) E(S); E(M(S); M) \hat{i}_{\text{sim}, w}(fSg_N)}{H_w(E; M; fSg_N)} \\ &= \frac{\sum_{S \in \mathbb{L}^d} f(S)}{\langle E; M \rangle} : \end{aligned} \quad (5)$$

Let  $A$  be a set of operators acting on configuration space  $\mathbb{L}^d$

$$A \subset fA : A \in \mathbb{S}^2_{\mathbb{L}^d} \otimes \mathbb{S}^2_{\mathbb{L}^d} g : \quad (6)$$

The transition observable  $N_A^{i,j}(S)$  is defined as the number of operators  $A \in A$  acting on the particular microstate  $S$ , which result in microstates  $S'$  with interaction energy  $E(S') = E(S) + i E$  and magnetization  $M(S') = M(S) + j M$ :

$$N_A^{i,j}(S) := \sum_{S' \in \mathbb{S}^2_{\mathbb{L}^d}} \mathbb{E}(S') \mathbb{E}(S) + i \mathbb{E}(M(S)) \mathbb{M}(S) + j \mathbb{M}(S) \in \mathbb{A}^2 \mathbb{A} : \quad (7)$$

(See Fig. 1 for an illustration of the thus defined observables.) Then, for any set of operators  $A$  which satisfies

$$0 \in \sum_{S' \in \mathbb{S}^2_{\mathbb{L}^d}} \mathbb{E}(S') \mathbb{E}(M(S)) N_A^{i,j}(S) = \sum_{S' \in \mathbb{S}^2_{\mathbb{L}^d}} \mathbb{E}(S') \mathbb{E} + i \mathbb{E}(M(S)) \mathbb{M} + j \mathbb{M} N_A^{i,j}(S) ; \quad (8)$$

the density of states  $(E; M)$  can be calculated from the microcanonical averages (5) of the thus defined transition observables to yield

$$(E; M) = \frac{\ln N_A^{i,j}(S) \ln(E + i E \mathbb{M} + j M)}{\ln N_A^{i,j}(S) \ln(E \mathbb{M})} : \quad (9)$$

Remarks:

1. Microreversibility as explained in App. A is a sufficient condition for the equality in (8). Apart from this condition which is implemented easily, the set  $A$  of operators can be chosen arbitrarily.
2. In the density of states, a multiplicative constant is physically irrelevant! For that reason,  $i$  can be chosen arbitrarily for one particular value of  $(E; M)$ . Then, the density of states of the remaining  $(E; M)$  values can be calculated from Eqn. (9).
3. The efficiency of the transition observable method depends crucially on the particular choice of  $A$ .
4. The transition observable method is neither restricted to the investigation of Ising systems (with bare next neighbour interaction, cf. [12]) nor to the investigation of discrete systems (cf. [13]). Example: consider a discrete spin system with a Hamiltonian consisting of two interaction terms

$$H(S) = E_1(S) + E_2(S) ; \quad (10)$$

which depends on certain coupling constants, say,  $J_1$  and  $J_2$  (e.g. ferromagnetic coupling to next neighbours and antiferromagnetic coupling to next-nearest neighbours). The knowledge of the density of states as a function of  $E_1$  and  $E_2$ , i.e.

$$(E_1; E_2) = \sum_{S \in \mathbb{S}^2_{\mathbb{L}^d}} \mathbb{E}_1(S) \mathbb{E}_1 + \mathbb{E}_2(S) \mathbb{E}_2 : \quad (11)$$

enables the determination of the thermodynamic properties of the system for all possible values of the ratio of the coupling constants by applying certain "skew-summing" techniques (cf. [14]). In complete analogy to the above, a set of transition observables can be defined, which facilitates the determination of the thus defined density of states  $(E_1; E_2)$ .

5. For a matrix  $T$  defined as

$$[T]_{(E^0; M^0); (E; M)} = \frac{1}{|A|} N_A^{\frac{E^0 - E}{E}, \frac{M^0 - M}{M}} (S) (E; M); \quad (12)$$

where  $|A|$  is the cardinality of the set  $A$ , it is easy to show that

a)  $T$  is a stochastic matrix, i.e.

$$[T]_{(E^0; M^0); (E^0; M^0)} = 1 \quad (13)$$

and

$$\sum_{(E^0; M^0)} [T]_{(E^0; M^0); (E; M)} = 1 \quad (14)$$

b) The density of states is the stationary state of  $T$ :

$$\sum_{(E; M)} [T]_{(E^0; M^0); (E; M)} (E; M) = (E^0; M^0); \quad (15)$$

Furthermore, if  $T$  is regular, i.e. if for all  $E^0; M^0$  and  $E; M$

$$\text{rank } N : [T^m]_{(E^0; M^0); (E; M)} > 0 \quad \forall m \geq n; \quad (16)$$

the stationary state of  $T$  is unique. Nevertheless, even if this condition is not fulfilled, the density of states can be computed piecewise on certain subsets  $E; M$  of the total set of possible energy and magnetization values of the system. The thus produced "fragments" of the density of states are then connected to each other via (a priori unknown) multiplicative constants.

Note here that the stochastic matrix  $T$  defined above is closely related to the so-called Transition Matrix Monte Carlo method introduced by Swendsen and Li [15].

E. Reduction to Oliveira's observable: the reduced transition observable method

The results of Sec. II D can be simplified to those presented by Oliveira in reference [5], where no information on the magnetization of the system is regarded. Formally, this can be achieved by a summation over the magnetization  $M$  (or the index  $j$ , respectively) in some of the expressions of the preceding section. Then, however, only a determination of the reduced density of states

$$\tilde{\rho}(E) = \frac{1}{M} \sum_{S \in \Omega} \delta(E - E(S)) \quad (17)$$

is feasible, which does not entail the entire thermodynamic information of the system (in the sense that  $\rho(E; M)$  enables the calculation of thermal and magnetic equations of state in various ensembles whereas  $\tilde{\rho}(E)$  just allows for the estimation of the thermal equation of state).

The reduced microcanonical average of any system observable  $f(S)$  over the energy shell  $E(S) = E$  is defined:

$$\langle f(S) \rangle_{\tilde{\rho}(E)} = \lim_{N \rightarrow \infty} \frac{\frac{1}{P} \sum_{S \in \Omega} \delta(E(S) - E) \sum_{i=1}^P f(S) g_N(S)}{\frac{1}{P} \sum_{S \in \Omega} \delta(E(S) - E) g_N(S)} = \frac{\int_{E(S) - E}^{E(S) + E} f(S) dS}{\tilde{\rho}(E)} : \quad (18)$$

We further define the reduced transition observable

$$\begin{aligned} \tilde{N}_A^i(S) &= \frac{1}{M} \sum_{S \in \Omega} \delta(S - S') \sum_{j=1}^{M-1} \delta(S' - S + j) = \\ &= \frac{1}{M} \sum_{S \in \Omega} \delta(S - S') \sum_{j=1}^{M-1} \delta(S' - S + j) : \end{aligned} \quad (19)$$

Then, for any set of operators  $A$  which satisfies

$$\frac{1}{M} \sum_{S \in \Omega} \delta(S - S') \tilde{N}_A^i(S) = \frac{1}{M} \sum_{S \in \Omega} \delta(S - S') \tilde{N}_A^i(S) ; \quad (20)$$

the reduced density of states (17) can be calculated from the reduced microcanonical average (18) of the reduced transition observable (19):

$$\tilde{\rho}(E + i\epsilon) = \frac{\tilde{N}_A^i(E + i\epsilon)}{\tilde{N}_A^i(E)} \tilde{\rho}(E) : \quad (21)$$

Again, microreversibility (cf. appendix A) is sufficient to ensure the equality in (20).

### III. COMPARISON OF THE EFFICIENCY OF THE STANDARD HISTOGRAM AND THE TRANSITION OBSERVABLE TECHNIQUE

To demonstrate the advantages of the transition observable method, numerical results obtained from either the standard histogram method or the transition observable method are compared. The philosophy of the comparison is to use some simulation technique to generate one sample of microstates which then is evaluated according to both methods. The simulations were performed for  $d = 2$ ,  $L = 32$  and  $d = 3$ ,  $L = 10$  Ising system. For the sake of completeness, the details of the computer simulations are given in App. C. The set  $A$  of lattice operators was chosen to consist of  $L^d$  operators, which are labelled by the subscript  $i$  and are defined by their action on a particular microstate  $S$ :

$$A_i : S = 1; 2; \dots; i; \dots; L^d \quad \mathcal{S} = 1; 2; \dots; i; \dots; L^d \quad (22)$$

i.e. the operator  $A_i$  acts only on the  $i$ -th spin of the Ising lattice. Obviously, since  $A_i A_i S = S$ , the thus defined set of operators meets the condition (A 2) and therefore is microreversible. Note that the determination of the simulation average of the transition observable by use of this particular set of lattice operators can be done very fast. In fact, the time needed for applying the  $L^d$  operators of the set  $A$  to a particular microstate is much shorter than the time needed to perform a lattice sweep!

Simulation averages of  $N_A^{i;j}$  were recorded only for values of  $i \in \{1, 0, 1\}$  and  $j \in \{1, 1\}$ .

To emphasize the difference between the two methods, we compare "discrete derivatives" (i.e. ratios of differences) of the logarithm of the density of states, namely:

(i) For the case of  $d = 2$  Ising model:

$$E \quad \ln \tilde{\rho}(E) = \frac{1}{2^E} \frac{\ln \tilde{\rho}(E + 1) - \ln \tilde{\rho}(E - 1)}{2} \quad (23)$$

$$= \frac{1}{2^E} \ln 4 \frac{hN_A^{1,1}(S) \tilde{\rho}(E + 1) - hN_A^{1,1}(S) \tilde{\rho}(E - 1)}{hN_A^{1,1}(S) \tilde{\rho}(E + 1) + hN_A^{1,1}(S) \tilde{\rho}(E - 1)} \quad (24)$$

(ii) For the case of  $d = 3$  Ising model:

$$M \quad \ln \tilde{\rho}(EM) = \frac{1}{2^M} \frac{4 \ln \tilde{\rho}(EM + 1) - 4 \ln \tilde{\rho}(EM - 1)}{4} \quad (25)$$

$$= \frac{1}{2^M} \ln 4 \frac{hN_A^{1,1,1}(S) \tilde{\rho}(EM + 1) - hN_A^{1,1,1}(S) \tilde{\rho}(EM - 1)}{hN_A^{1,1,1}(S) \tilde{\rho}(EM + 1) + hN_A^{1,1,1}(S) \tilde{\rho}(EM - 1)} \quad (26)$$

$$= \frac{1}{2^M} \ln 4 \frac{hN_A^{1,1,1}(S) \tilde{\rho}(EM + 1) - hN_A^{1,1,1}(S) \tilde{\rho}(EM - 1)}{hN_A^{1,1,1}(S) \tilde{\rho}(EM + 1) + hN_A^{1,1,1}(S) \tilde{\rho}(EM - 1)} \quad (27)$$

$$= \frac{1}{2^M} \ln 4 \frac{hN_A^{0,1,1}(S) \tilde{\rho}(EM + 1) - hN_A^{0,1,1}(S) \tilde{\rho}(EM - 1)}{hN_A^{0,1,1}(S) \tilde{\rho}(EM + 1) + hN_A^{0,1,1}(S) \tilde{\rho}(EM - 1)} \quad (28)$$

Note that both "discrete derivatives" (23) and (25) are closely related to microcanonical equations of state (see [9{11] and appendix B for more details].

A . Example 1: the  $d = 2$ ,  $L = 32$  Ising lattice

In Fig. 2, the differences of the logarithm of the reduced density of states as emerging from the transition observable method (cf. (24)) and the conventional histogram method

(cf. (4)) are shown together with the exact result [18]. By use of a sample of  $8 \cdot 10^5$  microstates, the transition observable method yields a result which, on the scale of the figure, can hardly be distinguished from the exact result, whereas the data obtained from the histogram method scatter strongly around the latter.

In Fig. 3, the results of the transition observable method (using one sample of  $n = 8 \cdot 10^5$  microstates) are compared to the results of the histogram method for several sample lengths ( $n, 5 \cdot n, 10 \cdot n$  and  $15 \cdot n$ ) by plotting the deviation of the simulation data from the exact result. Even if the simulation time is chosen 15 times longer in the histogram method, the transition observable method still yields more accurate results.

Calculating the mean square deviation of the simulation data from the exact result as a function of simulation time<sup>4</sup> (Fig. 4), we notice that the accuracy of both methods is improved according to a power law (the corresponding exponents seem to be the same ( $-1$ ) in both methods). But, at any given time, the transition observable method beats the standard histogram method in accuracy by a factor of roughly 40.

### B. Example 2: the $d = 3, L = 10$ Ising lattice

From the Monte Carlo samples, we computed the differences of the logarithm of the density of states in direction of the magnetization according to Eq. (4) in the case of the histogram method and according to Eqs. (26)–(28) in the case of the transition observable method (in fact, we computed the mean value of the three possibilities (26)–(28) of determining  $M(\ln)$ ).

In Figs. 5a) and b),  $M(\ln)$  is shown for  $E = 10^3 = -0.924$ . In Fig. 5a), a sample of length  $10 \cdot 10^5$  microstates is used for the evaluation of  $M(\ln)$  according to both methods whereas in Fig. 5b), the histogram method with a sample length of  $50 \cdot 10^5$  microstates is compared to the transition observable method with sample length  $10 \cdot 10^5$  again. For a better visualization of the difference between the two methods, an odd polynomial ( $f_{\text{fit}}(M) = aM + bM^3 + cM^5$ ) was fitted to the transition observable data. Subtraction of the data of Figs. 5a) and b) from this polynomial yields the plots shown in Figs. 5c) and d). In the figures, the transition observable (histogram) data are represented by the solid lines (points). The plots of the differences show the consistency of both methods, that is: both data sets scatter "randomly" around the  $t$  function. The data emerging from the transition observable method, however, are much more accurate than the data emerging from the standard histogram method even if much longer samples are used in the latter.

For a quantitative comparison between the two methods, the mean square deviations of the simulation results, with respect to a  $t^5$  to the best data obtained by the transition

<sup>4</sup>The comparison of the data was done within a certain "energy window" which was chosen around the centre of the histogram, i.e. the tails of the histogram have been discarded. Since the same sample is used in both evaluation techniques, the result of the comparison does not depend on the width of the "energy window" chosen for the evaluation of the  $t^2$ -deviations.

<sup>5</sup>We have performed a weighted  $t^2$  of an odd polynomial  $f_{\text{fit}}(M) = aM + bM^3 + cM^5$  to

observable method, is shown as a function of the simulation time in Fig. 6. The accuracy is improved according to a power law with exponent  $-1$  in both methods. But: at any given time, the transition observable method yields results which are more accurate than the results emerging from the histogram method by a factor  $1=250$  in the sense of the mean square deviation. In order to produce results of similar quality, the simulation time in the standard histogram method has to be 250 times longer than in the transition observable method!

### C. General remarks on section III

1. The two examples discussed in the preceding sections show that a simulation can be accelerated dramatically by use of the transition observable method. Here, it is not the algorithm to speed up the simulation but it is the observable measured during the simulation! The reason for this striking difference is indeed very simple: while every microstate, which is decided to be part of the sample, just yields one entry in a list in the histogram method, it might yield many transitions to neighbouring states (neighbouring with respect to the interaction energy and/or magnetization) and, hence, the statistics of the transition observable method can be expected to be much better than the statistics of the conventional histogram method. In fact, since the Ising system s under consideration just allows for 5 (7) different interaction energy changes and only two magnetization changes<sup>6</sup> under single spin flip operations (in  $d = 2$  (3)), the set of operators  $A$  chosen above can be expected to shorten the computational effort by a remarkable factor, roughly proportional to the square-root of the inverse volume  $L^{d=2}$  of the system!
2. The change of interaction energy under a single spin flip operation depends on the configuration of the spins in the very neighbourhood of the particular spin to be flipped. The typical configurations of neighbouring spins vary with the interaction energy of the whole system. For that reason, the factor of proportionality of the efficiency gain in the sense of the  $^2$ -comparison introduced above can be expected to depend on the mean interaction energy of the histogram, which itself depends on the simulation parameters (i.e. the stationary distribution).
3. The particular way of generating the sample of microstates is not important in the context of the comparison of the two methods introduced in Sec. II.

---

the data obtained from a  $50 \times 10$  sample by applying the transition observable method. The errors needed for the weighted fit have been produced by a jackknife blocking procedure using 25 data sets of length  $2 \times 10^6$  sweeps.

<sup>6</sup>  $E = J = (12); 8; 4; 0$  and  $M = 2$  in  $d = (3); 2$ .

#### IV . C O N C L U S I O N

A Monte Carlo simulation consists of two steps. The first step is the generation of a sample or spot check of microstates. The second step is the investigation of these microstates. Conventionally, if the aim is to speed-up the simulation, the first step is modified while the second remains unchanged. We have shown that a more extensive exploitation of the microstates of the sample, i.e. taking simulation averages of the transition observable instead of just cumulating a standard histogram, can effectively speed-up the simulation by a tremendous amount!

In an extremely straightforward implementation of the transition observable method, we reach a speed-up which can be expected to be proportional to the square root of the volume  $L^d$  of the system under consideration. Such a speed-up seems unattainable by an improvement of the algorithm of the simulation, i.e. by modifying the first step of the simulation.

Even though the transition observable method seems to be built for discrete spin systems, one of us (J.D. M unoz, cf. [13]) has already shown that the method can be transferred to continuous spin systems.

An extension of this method to "non-spin" systems like polymers might be a topic of future investigations.

#### A C K N O W L E D G M E N T S

We would like to thank A. Huller for valuable discussions and P.M.C. de Oliveira for some remarks on the history of the Broad Histogram Method cited in Refs. [4], [5] and [6]. One of us (J.D. Munoz) would like to thank H.J. Herrmann for hospitality and the Deutscher Akademischer Austauschdienst for financial support through scholarship A/96/0390.

#### A P P E N D I X A : M I C R O R E V E R S I B I L I T Y

Let  $A$  be a set of operators acting on configuration space  $L^d$

$$A \quad fA : AS \subset L^d \quad 8 S \subset L^d \quad (A1)$$

such that for all  $A \in A$ , there exists a unique inverse operator  $B = A^{-1} \in A$ , i.e.

$$8A \in A \quad 9! B \in A : B A S = S : \quad (A2)$$

Then,  $A$  is said to show microreversibility.

From the microreversibility of  $A$ , it follows immediately that the number of operators  $A \in A$  which transforms  $S$  into  $S'$  equals the number of operators  $A \in A$  which transform  $S'$  back into  $S$ , i.e.

$$\frac{X}{AS, S'} = \frac{X}{S, A S'} : \quad (A3)$$

Using the definition of the transition observable (7), this can be shown to be equivalent to

$$\frac{X}{S^2} \frac{E(S); E - M(S); M}{L^d} N_A^{i,j}(S) = \frac{X}{S^2} \frac{E(S); E + iE - M(S); M + jM}{L^d} N_A^{i,j}(S) : \quad (A4)$$

That is, the number of operations which transform microstates with interaction energy  $E$  and magnetization  $M$  into microstates with  $E + iE$  and  $M + jM$  by use of operators  $A \rightarrow A$  is identical to the number of operations which transform "backwards", i.e. from states with  $E + iE$  and  $M + jM$  to those with interaction energy  $E$  and magnetization  $M$ .

#### APPENDIX B : MICROCANONICAL EQUATIONS OF STATE

As mentioned in Secs. III, the differences of the logarithm of the density of states  $\ln \rho_m$  are related to the microcanonical magnetic equation of state. Indeed, equation (25) is the microcanonical magnetic equation of state in a discrete notation (appropriate for the description of finite Ising systems), which converges in the thermodynamic limit  $L \rightarrow \infty$  towards the magnetic equation of state of the infinite system

$$\frac{h}{T}(\beta; m) = \frac{\partial}{\partial m} \lim_{L \rightarrow \infty} L^d \ln (\rho(E; M; L^d)) ; \quad (B1)$$

where  $\beta = L^d E$  and  $m = L^d M$  are intensive quantities. The difference of the logarithm of the reduced density of states, as defined in Eq. (23), converges towards  $(\beta; h=0)$  of the infinite system for zero external field and can serve to compute zero field properties of the system<sup>7</sup>.

Note that it is unnecessary and a rather roundabout way to convert the thus obtained data into the commonly used canonical quantities. For details on the investigation of phase transitions in a microcanonical approach and a microcanonical finite-size scaling theory see references [9], [10] and [11].

#### APPENDIX C : DETAILS OF THE MONTE CARLO SIMULATION

##### 1. Simulation of the $d = 2$ , $L = 32$ Ising lattice

A Monte Carlo simulation of a  $32^2$  Ising system with periodic boundary conditions was performed. The stationary distribution of the underlying Markov-process was chosen to be proportional to the Boltzmann weight  $w(E(S); M(S)) / \exp(-H(S)/T)$  with simulation parameters  $h = 0$  and  $T = 2.269$  (see Sec. II A for the definition of the Ising Hamiltonian). We have implemented a sequential lattice update with a "Metropolis-type" transition rate  $T(S \rightarrow S') = m \ln f_1(S') - f_1(S)$  and we have sampled every  $L^2$  configuration only. After "equilibration" (64  $10^6$  lattice sweeps have been discarded), several successive samples of  $8 \cdot 10^6$  microstates were taken.

---

<sup>7</sup>  $(\beta; h=0)$  is the derivative with respect to  $\beta$  of the Legendre transform of  $\lim_{L \rightarrow \infty} L^d \ln (\rho(\beta; m; L^d))$  with respect to  $m$ .

## 2. Simulation of the $d = 3$ , $L = 10$ Ising lattice

A Monte Carlo simulation of a  $10^3$ -Ising system with periodic boundary conditions was performed. The stationary distribution was chosen to be  $w(E(S);M(S)) \propto f(E_0, E(S)) \propto N_0 g^{(N_0/2)-2}$ , i.e., independent of  $M(S)$  again. The parameters were chosen to be  $E_0 = 1586$  and  $N_0 = 1000$  (for a detailed discussion and interpretation of this stationary distribution, see [19]). The way of updating the lattice configurations is the same as for the simulation of the  $32^2$ -Ising system (cf. App. C 1). After "equilibration" ( $2 \times 10^6$  lattice sweeps have been discarded), several successive samples of  $2 \times 10^4$  microstates were taken.

## REFERENCES

- [1] Z.W. Salsburg, J.D. Jacobson, W. Fickett, W.W. Wood, *J. Chem. Phys.* 30, 65 (1959)
- [2] A.M. Ferrenberg, R.H. Swendsen, *Phys. Rev. Lett.* 61, 2635 (1988)
- [3] R.H. Swendsen, *Physica A* 194, 53 (1993)
- [4] In the original work [5], Oliveira presented the transition observable method together with a new simulation technique. Unfortunately, the part concerning the simulational aspects contains some errors which were suspected by Berg and Hansmann [7], and explicitly pointed out as well as corrected by Wang [8]. In this paper, the transition observable method is formulated independent of (any) simulation technique.
- [5] P.M.C. de Oliveira, T.J.P. Penna, H.J. Hermann, *Braz. J. of Phys.* 26, 677 (1996), also in cond{m at/9610041
- [6] P.M.C. de Oliveira, T.J.P. Penna, H.J. Hermann, *Eur. Phys. J. B* 1, 205 (1998)
- [7] B.A. Berg, U.H.E. Hansmann, *Eur. Phys. J. B* 6, 395 (1998)
- [8] J.-S. Wang, *Eur. Phys. J. B* 8, 287 (1999);  
J.-S. Wang, L.W. Lee, cond{m at/9903224.
- [9] M.Kastner, M.Promberger, A.Huller, in *Computer Simulation Studies in Condensed Matter Physics XI*, edited by D.P.Landau, H.-B.Schuttler, Heidelberg (1998)
- [10] M.Kastner, M.Promberger, A.Huller, in preparation
- [11] M.Promberger, M.Kastner, A.Huller, cond{m at/9904265
- [12] A.R.Lima, P.M.C.de Oliveira, T.J.P.Penna, in preparation
- [13] J.D.Munoz, H.J.Hermann, *J. Mod. Phys. C* 10, 95 (1999);  
J.D.Munoz, H.J.Hermann, in *Computer Simulation Studies in Condensed Matter Physics XII*, edited by D.P.Landau, S.P.Lewis, and H.-B.Schuttler, Springer Verlag, Heidelberg, Berlin (1999)
- [14] M.Deserno, *Phys. Rev. E* 56, 5204 (1997)
- [15] R.H. Swendsen, Shing{Te Li, unpublished, see also [16] and [17]
- [16] J.-S. Wang, T.K.Tay, R.H. Swendsen, *Phys. Rev. Lett.* 82, 476 (1999)
- [17] J.-S. Wang, cond{m at/9810240
- [18] P.D. Beale, *Phys. Rev. Lett.* 76, 78 (1996)
- [19] A.Huller, R.W.Gerling, *Z. Phys. B* 90, 207 (1993)



FIGURES

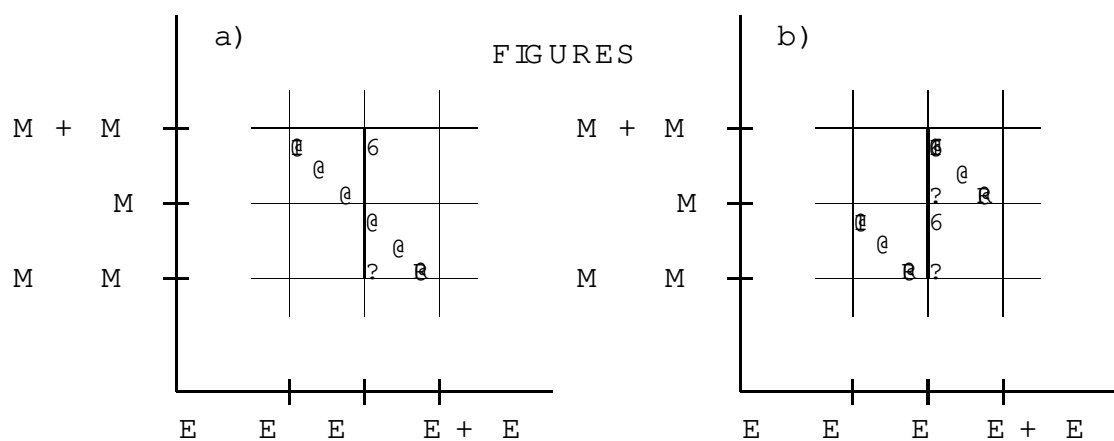


Figure 2:

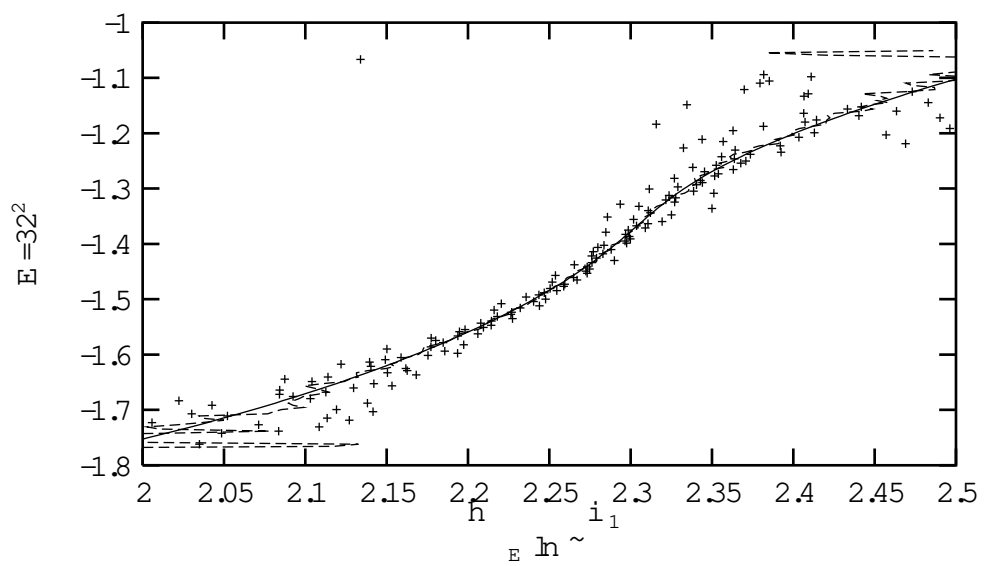


Figure 3:

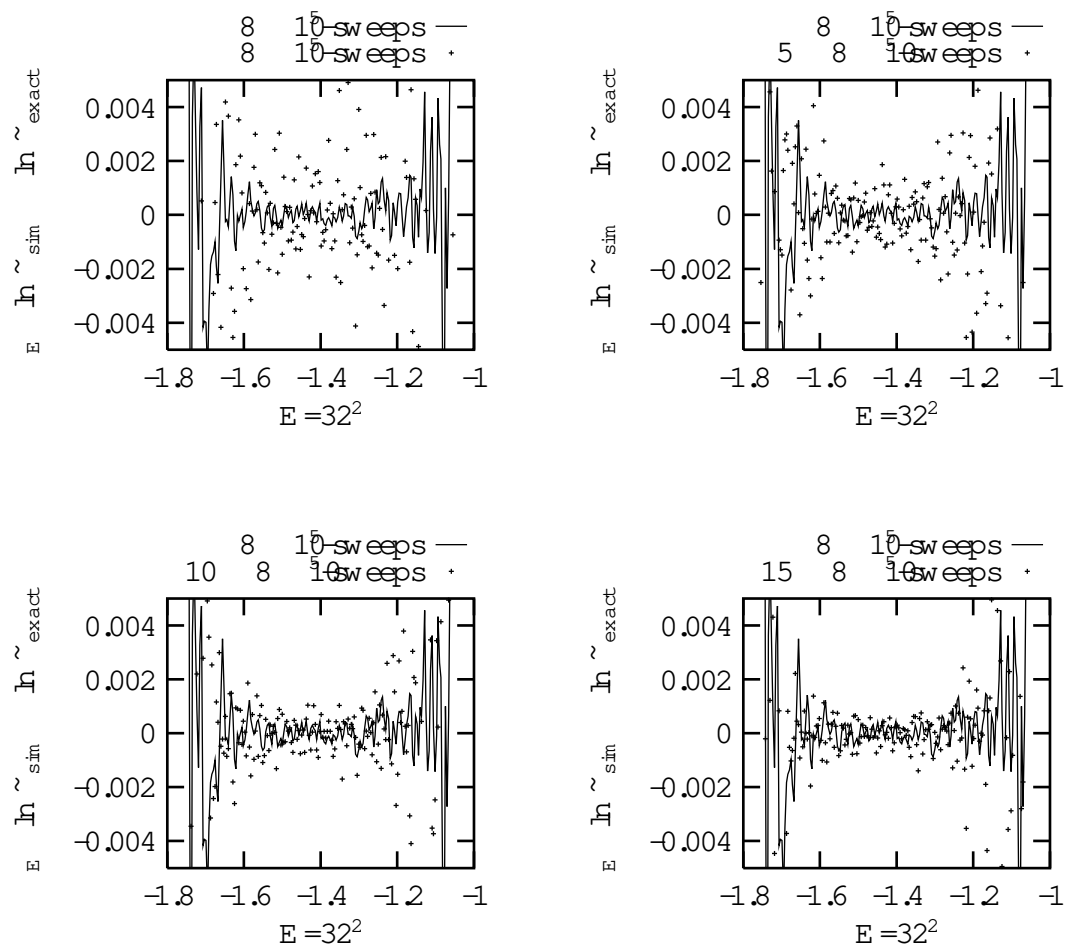


Figure 4:

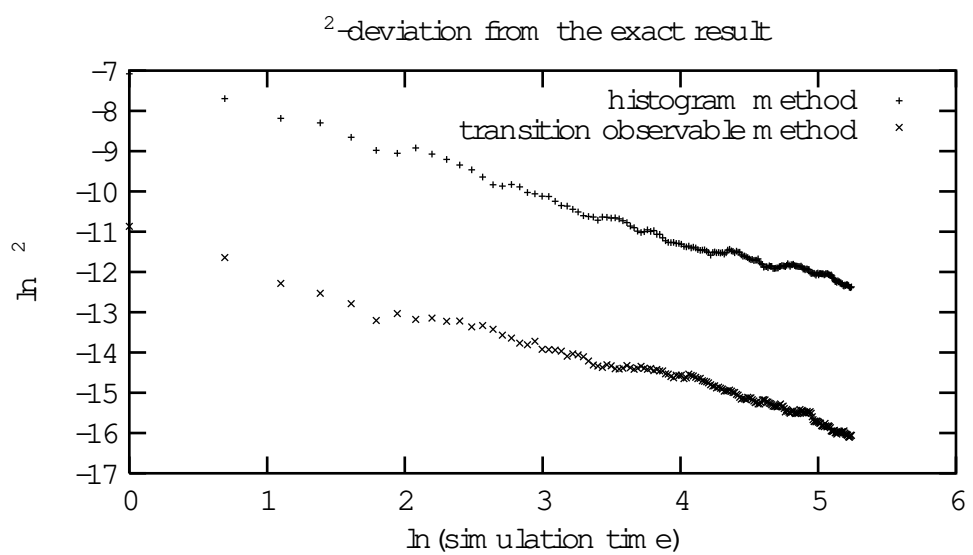


Figure 5:

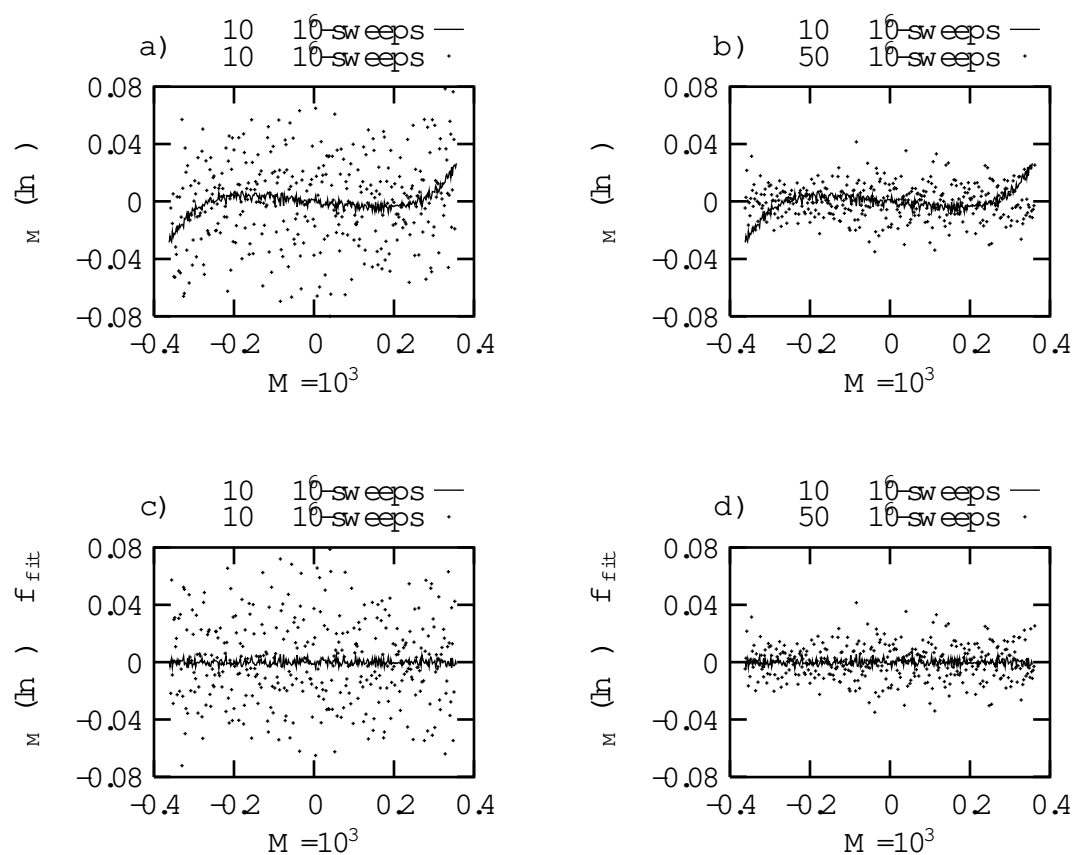
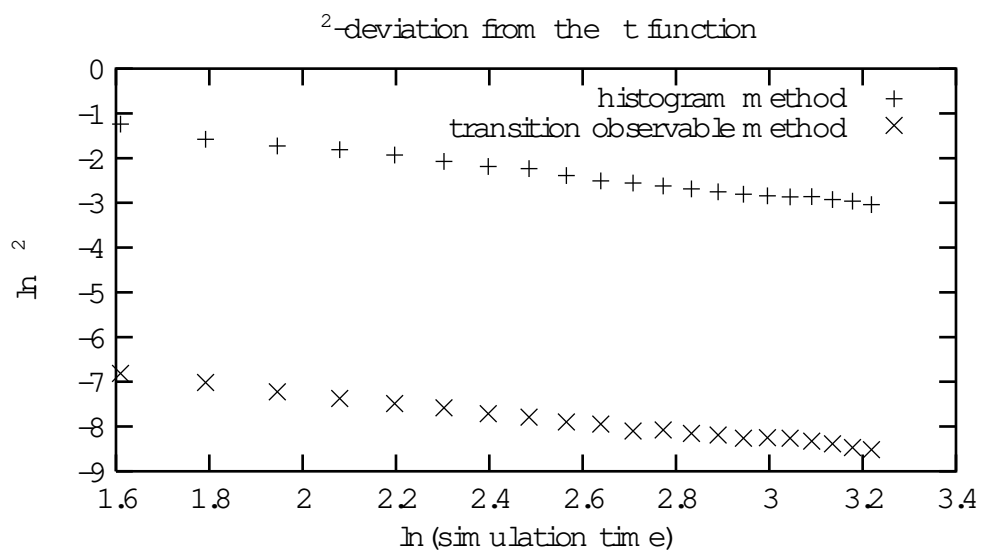


Figure 6:



C aptions:

FIG . 1. a) Visualization of the transition variables  $N_A^{i,j}$  for the case  $i \in \{0, 1\}$  and  $j \in \{0, 1\}$ . Given a particular microstate  $S$  with interaction energy  $E(S) = E$  and magnetization  $M(S) = M$ ,  $N_A^{i,j}(S)$  gives the number of possibilities to reach any state  $S'$  with energy  $E(S') = E(S) + i \cdot E$  and magnetization  $M(S') = M(S) + j \cdot M$  by applying the set of lattice operators  $A$  to the microstate  $S$ . The microcanonical average of the transition observable  $N_A^{i,j}$  is proportional to the total number of possibilities for the event that, given any state  $S$  with energy  $E(S) = E$  and magnetization  $M(S) = M$ , any other state  $S'$  with energy  $E(S') = E(S) + i \cdot E$  and magnetization  $M(S') = M(S) + j \cdot M$  is reached under the action of  $A$ . Fig. 1b) shows the "transition paths" corresponding to the various microcanonical expectation values contributing to the differences of the logarithm of the density of states  $\ln \rho(E; M)$  at the point  $(E; M)$ , as introduced in Sec. III.

FIG . 2. Intensive energy as a function of  $E \ln \rho(E; M)$  of a  $32^2$  square Ising system. The solid line is the exact result, the dashed line corresponds to the transition observable method and the points to the conventional histogram method. The same sample of  $8 \cdot 10^4$  microstates was used to perform both evaluations. The energy is plotted against  $E \ln \rho(E; M)$  because of its correspondence to a thermalequation of state  $E(T)$ ; cf. App. B. The strong fluctuations in both the high energy and the low energy region of the figure are due to poor statistics in the tails of the histograms. In the central region, the difference between the dashed and the full line is smaller than the line thickness!

FIG . 3. In order to point out the differences between the transition observable method and the conventional histogram method and in order to show that the used estimators are indeed unbiased, the data emerging from the Monte Carlo simulation are subtracted from the exact result. The transition observable data (histogram data) are represented by solid lines (points).

FIG . 4. In order to judge the quality of the two methods, the  $\chi^2$ -deviation of the simulation results from the exact result is shown as a function of the simulation time (in units of  $8 \cdot 10^4$  lattice sweeps).

FIG . 5. a) and b): differences of the logarithm of the density of states  $\ln \rho(E; M)$  for  $E = 10^3 = 0.924$ . In Fig. a), a sample of length  $10^5$  microstates is used for the evaluation of  $\ln \rho(E; M)$  according to both methods whereas in Fig. b), the histogram method with a sample length of  $50 \cdot 10^4$  microstates is compared to the transition observable method with sample length  $10^5$  again. For a better demonstration of the difference of the two methods, the same data are subtracted from a  $t$  function in Fig. c) and d) (see text for the details of the  $t$ ). In all figures, the transition observable data (histogram data) are represented by the solid lines (points).

FIG . 6. In order to compare the quality of the results emerging from the histogram method to those emerging from the transition observable method, the mean square deviations of the simulation results with respect to a fit to the best data obtained by the transition observable method is shown as a function of the simulation time (in units of  $2 \times 10^6$  lattice sweeps).